CORE
Metadata, citation and similar papers at core.ac.uk
Provided by Elsevier - Publisher Connector

Biochimica et Biophysica Acta 1817 (2012) 1191–1195

Contents lists available at SciVerse ScienceDirect

Biochimica et Biophysica Acta

journal homepage: www.elsevier.com/locate/bbabio

Cationic state distribution over the chlorophyll *d*-containing P_{D1}/P_{D2} pair in photosystem II☆

Keisuke Saito [a], Jian-Ren Shen [b], Hiroshi Ishikita [a,c,*]

[a] 202 Building E, Career-Path Promotion Unit for Young Life Scientists, Graduate School of Medicine, Kyoto University, Yoshida-Konoe-cho, Sakyo-ku, Kyoto 606-8501, Japan
[b] Division of Bioscience, Graduate School of Natural Science and Technology/Faculty of Science, Okayama University, Okayama 700-8530, Japan
[c] Japan Science and Technology Agency (JST), PRESTO, 4-1-8 Honcho Kawaguchi, Saitama 332-0012, Japan

ARTICLE INFO

Article history:
Received 18 October 2011
Received in revised form 2 December 2011
Accepted 6 December 2011
Available online 13 December 2011

Keywords:
Photosystem II
Chlorophyll *d*
Spin density distribution
Acaryochloris marina
Redox potential
P680

ABSTRACT

Most of the chlorophyll (Chl) cofactors in photosystem II (PSII) from *Acaryochloris marina* are Chl*d*, although a few Chl*a* molecules are also present. To evaluate the possibility that Chl*a* may participate in the P_{D1}/P_{D2} Chl pair in PSII from *A. marina*, the $P_{D1}^{\bullet+}/P_{D2}^{\bullet+}$ charge ratio was investigated using the PSII crystal structure analyzed at 1.9-Å resolution, while considering all possibilities for the Chl*d*-containing P_{D1}/P_{D2} pair, i.e., Chl*d*/Chl*d*, Chl*a*/Chl*d*, and Chl*d*/Chl*a* pairs. Chl*d*/Chl*d* and Chl*a*/Chl*d* pairs resulted in a large $P_{D1}^{\bullet+}$ population relative to $P_{D2}^{\bullet+}$, as identified in Chl*a*/Chl*a* homodimer pairs in PSII from other species, e.g., *Thermosynechococcus elongatus* PSII. However, the Chl*d*/Chl*a* pair possessed a $P_{D1}^{\bullet+}/P_{D2}^{\bullet+}$ ratio of approximately 50/50, which is in contrast to previous spectroscopic studies on *A. marina* PSII. The present results strongly exclude the possibility that the Chl*d*/Chl*a* pair serves as P_{D1}/P_{D2} in *A. marina* PSII. This article is part of a Special Issue entitled: Photosynthesis Research for Sustainability: from Natural to Artificial.

© 2011 Elsevier B.V. All rights reserved.

1. Introduction

The reaction center of photosystem II (PSII) is composed of a D1/D2 heterodimer, harboring the chlorophyll *a* (Chl*a*) pair P_{D1}/P_{D2}, the accessory Chl*a* Chl_{D1}/Chl_{D2}, two pheophytin *a* $Pheo_{D1}/Pheo_{D2}$, two quinones, and two additional Chl*a* $Chl_{Z(D1)}/Chl_{Z(D2)}$ molecules as redox active cofactors. P680, which absorbs light at a wavelength of 680 nm, is formed among these Chl*a* molecules. Excitation of P680 leads to the formation of the $Chl_{D1}^{\bullet+}$ $Pheo_{D1}^{\bullet-}$ state [1–3], followed by the $[P_{D1}/P_{D2}]^{\bullet+}$ $Pheo_{D1}^{\bullet-}$ state. The resulting $[P_{D1}/P_{D2}]^{\bullet+}$ state serves as an electron abstractor for the oxygen-evolving complex (OEC). Thus, water oxidation is ultimately achieved by the high redox potential for one-electron oxidation (E_m) of P680. To date, the E_m(P680) value has not been directly measured in experimental studies. Instead, the E_m(P680) value has been estimated mainly from measured E_m values of other cofactors. The E_m(P680) value was first estimated to be 1.1 V by Klimov et al. in 1979 on the basis of the E_m value of pheophytin, measured as −0.61 V at pH 11 [4]. Subsequently, Rutherford et al. supported this claim, also estimating that the E_m(P680) value was 1.1 V [5]. In contrast, very low E_m(P680) values, between 0.8 and 0.9 V, were reported by Watanabe, Kobayashi, and colleagues [6–8]. After the PSII crystal structure from *Thermosynechococcus elongatus* was reported with 3.8-Å resolution [9], Rappaport et al. estimated that the E_m(P680) was 1.26 V [10], based on measurement of the $E_m(Q_A)$ (approximated to be −30 mV by Rutherford, Krieger, and colleagues [11,12]) in PSII from *Synechocystis* PCC 6803 [10]. This measurement was higher than previously reported [4,5]. In 2005, Grabolle and Dau reported a similar value of 1.25 V [13]. On the basis of the PSII crystal structure at 3.0-Å resolution [14], Ishikita et al. reported $E_m(P_{D1})$ and $E_m(P_{D2})$, .i.e., E_m for the Chl*a* monomer, to be 1.1–1.2 V by solving the linearized Poisson–Boltzmann equation and considering the protonation states of all titratable sites [15]. Recently, Kato et al. reported that the E_m(P680) was 1.17–1.21 V, extrapolated from an $E_m(Pheo_{D1})$ value of −0.5 V [16] measured at physiological pH (6.5) in PSII from *T. elongatus*. From these studies, it appears that the E_m(P680) value reaches 1.1–1.2 V (reviewed in Refs. [17–20]), a value significantly higher than the E_m of monomeric Chl*a* in organic solvents.

Following initial charge separation in the reaction center of PSII, the positive charge is distributed over P_{D1}/P_{D2}, resulting in a $P_{D1}^{\bullet+}/P_{D2}^{\bullet+}$ state. The $P_{D1}^{\bullet+}/P_{D2}^{\bullet+}$ ratio (or the corresponding spin density distribution) was reported to be 82/18 from ENDOR studies of spinach PSII [21] or 80/20 from flash-induced spectroscopic studies of *Synechocystis* PCC 6803 PSII [22], suggesting a preferential localization of the cationic state on P_{D1} over P_{D2}, irrespective of the high similarity in D1 and D2 protein sequences [23]. The cause of the asymmetric distribution of the cationic state has been attributed mainly to the electrostatic asymmetry of the

Abbreviations: *A. marina*, *Acaryochloris marina*; Chl, chlorophyll; OEC, oxygen-evolving cluster; PSII, photosystem II; QM/MM approach, quantum mechanical/molecular mechanical approach; *T. elongatus*, *Thermosynechococcus elongatus*; *T. vulcanus*, *Thermosynechococcus vulcanus*.

☆ This article is part of a Special Issue entitled: Photosynthesis Research for Sustainability: from Natural to Artificial.

* Corresponding author. Tel./fax: +81 75 753 9286.
E-mail address: hiro@cp.kyoto-u.ac.jp (H. Ishikita).

0005-2728/$ – see front matter © 2011 Elsevier B.V. All rights reserved.
doi:10.1016/j.bbabio.2011.12.003

D1/D2 residue pairs due to the presence of the OEC and associated functions in the D1 protein subunit side (secondary to the geometrical asymmetry of P_{D1}/P_{D2} chlorophylls) [24]; this is in contrast to the cationic state distribution of the corresponding Chl pair in PSI [25].

Chl*d* is the major Chl pigment in *Acaryochloris marina* (making up more than 95% of the Chl pigments), although some Chl*a* (less than 5%) is also present [26–29]. In *A. marina* grown under high iron conditions, the pigment content per 2 pheophytin *a* (i.e., $Pheo_{D1}$ and $Pheo_{D2}$) was estimated to be 1.4 Chl*a* [29]. Recent studies have suggested that the pigment stoichiometry of 2 pheophytin *a* in the *A. marina* PSII comprises 29.6 ± 1.2 Chl*d* and 1.9 ± 0.1 Chl*a* molecules [30]. Although the majority of the Chl is Chl*d*, characteristic for the *A. marina* PSII, the origin of the minor Chl (Chl*a*) is a serious question. Chl*d* and Chl*a* differ geometrically in their chemical group at the $C3^1$ atom position; Chl*d* possesses a formyl group at this position, whereas Chl*a* possesses a vinyl group (Fig. 1).

There is no direct evidence demonstrating that Chl*a* is actually located in the reaction center of the *A. marina* PSII (see statements in Ref. [31]). However, observation of the accumulation of the cationic state on a single Chl*a* molecule (i.e., bleaching at 435 nm and increase in absorption at 820 nm) in *A. marina* PSII by Schlodder et al. [31] should be considered, particularly in terms of the fact that prior studies have shown the accumulation of a cationic state specifically at P_{D1} in PSII from spinach [21], *Synechocystis* PCC 6803 [22], and *T. elongatus* [32,33]. Thus, Schlodder et al. proposed that P_{D1}/P_{D2} is a Chl*a*/Chl*d* heterodimer [31,34]. In addition, Cser et al. [35] concluded that the measured $E_m(Pheo_{D1})$ value in the *A. marina* PSII was the same as that in Chl*a* type PSII and proposed that Chl*a* was involved in the primary donor of the *A. marina* PSII. To unambiguously confirm this, however, one must clarify how the P_{D1}/P_{D2} moiety of the *A. marina* PSII is able to discriminate between the minor species Chl*a* and the major species Chl*d* and specifically uptake a Chl*a* molecule at the P_{D1} position.

On the other hand, Tomo et al. proposed that P_{D1}/P_{D2} is a Chl*d*/Chl*d* homodimer [36,37]. An advantage of the Chl*d*/Chl*d* homodimer model is that Chl*d* is the major species in the *A. marina* PSII, and thus, this model does not have to rationalize the specificity of Chl*a* at P_{D1}. In contrast to the results by Cser et al. [35], Tomo et al. [36] or Allakhverdiev et al. [38] observed that $E_m(Pheo_{D1})$ in the *A. marina* PSII was by ~80 mV higher than in the *Synechocystis* PCC 6803 PSII. Interestingly, the experimentally measured E_m value for Chl*d* in DMF is ~70 mV higher than that of Chl*a* [39]. The essentially same shift as observed in the $E_m(Pheo_{D1})$ difference between the two PSII proteins suggests the energetic conservation of light-induced charge separation and water oxidation among PSII species including the Chl*d*-containing P_{D1}/P_{D2} pair, preferring the Chl*d*/Chl*d* homodimer model over the Chl*a*/Chl*d* heterodimer model [38]. To support the Chl*d*/Chl*d* homodimer model, the researchers also presented light-induced Fourier transform infrared (FTIR) spectra of both the *A. marina* PSII and the *Synechocystis* PCC 6803 PSII [36]. The 1100–1800 cm^{-1} region of the *A. marina* PSII clearly indicates that approximately 80% of the cationic state was localized on a single Chl. Based on the high similarity of the D1/D2 protein sequences between the *A. marina* PSII and, for instance, the *T. elongatus* PSII (Fig. S1, supporting information), the cationic state is likely to be more populated on P_{D1} than P_{D2}. Thus, one can conclude that the $P_{D1}^{\bullet+}/P_{D2}^{\bullet+}$ ratio is approximately 80/20 for the *A. marina* PSII, as observed in PSII from spinach [21], *Synechocystis* PCC 6803 [22], and *T. elongatus* [32,33]. Because the CH stretching vibration of a formyl group corresponds to a peak at approximately 2700 cm^{-1} (see Refs. [36,40,41] and Refs. therein), it would be helpful to investigate this region to distinguish between Chl*a* and Chl*d* in P_{D1}/P_{D2}. However, the absorbance in this region is approximately 10 times weaker than that of the 1100–1800 cm^{-1} region of the *A. marina* PSII [36] (and also in the *A. marina* PSI [40,41]), making it difficult to assess and adding to the debate on P_{D1}/P_{D2} Chl models in the *A. marina* PSII.

All of these debates ultimately arise from the lack of structural information for the *A. marina* PSII. The exact molecular geometry surrounding the P_{D1}/P_{D2} Chl in the *A. marina* PSII remains unknown due to the lack of a crystal structure. Since the *A. marina* PSII possesses a high degree of D1 and D2 protein sequence similarity to the *T. vulcanus* PSII or the *T. elongatus* PSII (Fig. S1, supporting information), we investigated the relationship between a possible Chl pair at the P_{D1}/P_{D2} position (i.e., Chl*d*/Chl*d*, Chl*a*/Chl*d*, and Chl*d*/Chl*a*) and the cationic state charge distribution over the P_{D1}/P_{D2} pair, using the *T. vulcanus* PSII crystal structure analyzed at a 1.9-Å resolution [42]. To calculate the $P_{D1}^{\bullet+}/P_{D2}^{\bullet+}$ ratio for the P_{D1}/P_{D2} Chl dimer, we used a large-scale quantum mechanical/molecular mechanical (QM/MM) approach, with the explicit treatment of the complete PSII atomic coordinates, defining the P_{D1}/P_{D2} dimer as the QM region and the remaining protein subunits–cofactors

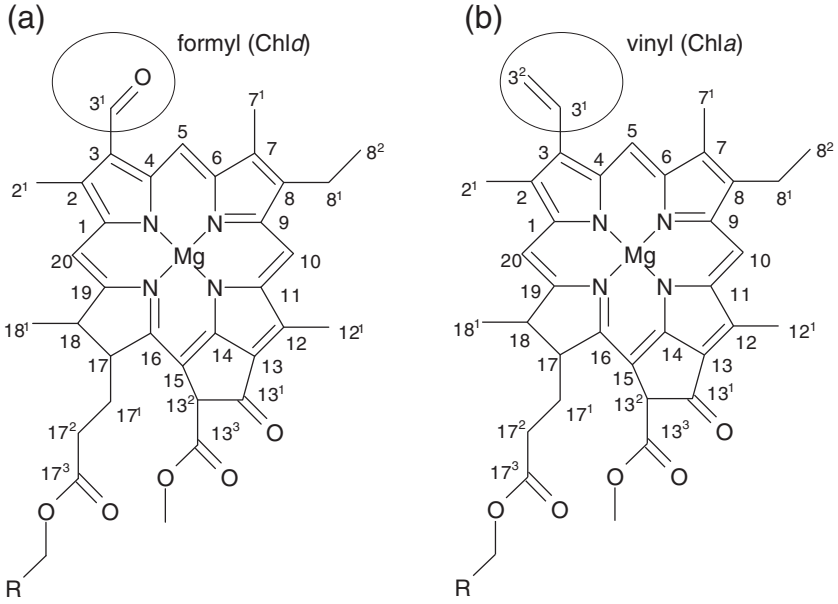

Fig. 1. Structure of (a) Chl*d* and (b) Chl*a* using the IUPAC numbering scheme (R = phytol chain).

as the MM region. Thus, the entire P_{D1}/P_{D2} molecule is considered quantumchemically in the presence of the PSII electrostatic protein environment.

To avoid an uncertain prediction of the protein structure, we used the original protein atomic coordinates of the *T. vulcanus* PSII crystal structure [42], without performing homology modeling for the *A. marina* PSII. The present results should be interpreted within this limiting condition. Nevertheless, the present procedure is currently the best option for investigating this phenomenon in the absence of high-resolution crystal structures of the *A. marina* PSII. Although the identity of the amino acid sequence of the D1 protein, e.g., the region at 191 to 210 near the axial ligand of P_{D1} (i.e., D1-His198) is 80%, not specifically high, there is essentially no significant difference in their electrostatic characters (e.g., no [charged residue]/[uncharged residue] difference at the corresponding position in the two D1 proteins), which will not affect the $P_{D1}^{\bullet+}/P_{D2}^{\bullet+}$ energetics. Indeed, it has been suggested that the structure of the *A. marina* PSII reaction center is similar to the PSII in Chl*a* organisms (see Ref. [31] and Refs. therein). In the *A. marina* PSII, delayed fluorescence from Chl*a* was observed as a result of charge recombination [36,43], which may suggest that Chl_{D1} should be also investigated together with P_{D1}/P_{D2} (i.e., in terms of Chl_{D1} as an initial donor in PSII [1–3]). Due to the large system size, we did not include Chl_{D1} and Chl_{D2} in the QM region. Nevertheless, to the best of our knowledge, this is the first study that clearly demonstrates the cationic charge distribution and spin density distribution over all possible combinations of Chl*d* and/or Chl*a* pairs at the P_{D1}/P_{D2} position in the PSII protein environment.

2. Methods

As demonstrated in the previous article [24,25], we employed the following systematic modeling procedure: We constructed a realistic molecular model of the whole PSII complex using the recent high-resolution crystal structure. To obtain deeper insight into the electronic structure of P_{D1}/P_{D2} Chl dimer, which is the key molecule of the photosystem II reaction center, we performed large-scale QM/MM calculations for the entire PSII complex. Technical details of each modeling procedure are identical to those used in previous studies on PSII [24] and PSI [25] and summarized as follows.

2.1. Coordinates

The atomic coordinates of PSII were taken from the X-ray structure of the PSII complexes from *T. vulcanus* at 1.9 Å resolution (PDB ID: 3ARC) [42]. Hydrogen atoms were generated and energetically optimized with CHARMM [44], whereas the positions of all non-hydrogen atoms were fixed, and all titratable groups were kept in their standard protonation states, i.e., acidic groups were ionized and basic groups were protonated. For the QM/MM calculations, we added additional counter ions to neutralize the whole system. To avoid unnecessary artifacts of the protein side chain geometry, we used the original protein atomic coordinates of the *T. vulcanus* PSII crystal structure [42], without performing homology modeling of the *A. marina* PSII. Accordingly, atomic coordinates of the cofactors expect for the P_{D1}/P_{D2} Chl pair were kept as in the original *T. vulcanus* PSII crystal structure.

2.2. Atomic partial charges

Atomic partial charges of the amino acids were adopted from the all-atom CHARMM22 [45] parameter set. The charges of the protonated acidic O atoms were increased symmetrically by +0.5 unit charges to implicitly account for the presence of a proton. Similarly, instead of removing a proton in the deprotonated state, the charges of all of the protons of the basic groups of Arg and Lys were diminished symmetrically by a total unit charge. For residues for which the protonation states were not available in the CHARMM22 parameter set, appropriate charges were computed [46]. For the cofactors (e.g., the OEC cluster, Chl*a*, Pheo*a*, and quinones), the same atomic charges as in previous computations of PSII [24] were used.

2.3. OEC models

In the S_1-state, the valences of the 4 Mn atoms are most probably (III, III, IV, and IV). The exact valences of the individual Mn atoms are unclear; however, we found that changing the charge distribution of each Mn atom from the above distribution did not affect our calculation results significantly [24]. The protonation states of the O atoms (and thus the net charge of the OEC atoms) in the OEC cluster remain unclear. Although O1, O2, and O3 are likely to be unprotonated O^{2-} based on observations of the OEC geometry, the protonation states of O4 linking Mn3 and Mn4 in the Mn_3CaO_4-cubane, and O5 in one of the corners of the cubane linking Mn4 and the cubane, necessitate more deep investigation as they might be O^{2-}, protonated OH^-, or even H_2O. Due to the uncertainty, we evaluated all possible combinations of the O4 and O5 protonation states and we tentatively used the $O4H^-$ $O5H^-$ model (see Ref. [24] for further details).

Except for a few examples [47], the spin coupling of the Mn ions has not been considered in a number of studies where the PSII protein environment was explicitly modeled (e.g., recent QM/MM studies on the S1-state model of OEC by Batista, Brudvig, and coworkers [48]). In particular, (i) our focus is not on the OEC cluster, (ii) the OEC cluster was included in the MM region (see below [24]), and (iii) the atomic charges of OEC do not differ significantly among the different spin structures [47]. Thus, the spin coupling was not considered in the present study.

2.4. QM/MM calculations

In all QM/MM calculations reported here, we employed the so-called electrostatic embedding QM/MM scheme. In all QM/MM calculations, we used the Qsite [49] program code. Electrostatic as well as steric effects created by complex PSII architecture were explicitly considered in all present calculations. Due to the large system size of PSII, the QM region was limited to the P_{D1}/P_{D2} Chl dimer for simplicity, while other protein units and all co-factors were approximated by the MM force field. Since we have optimized the atomic partial charges for the OEC cluster, Chl*a*, Pheo*a*, and quinones, the present QM/MM partition was accurate enough to describe the electronic structure of the $[P_{D1}/P_{D2}]^{\bullet+}$ Chl dimer. To reliably determine the cationic character of $[P_{D1}/P_{D2}]^{\bullet+}$ Chl dimer, we employed the unrestricted DFT method with the B3LYP functional and LACVP* basis sets. The detailed geometry of $[P_{D1}/P_{D2}]^{\bullet+}$ Chl dimer was refined by the constrained QM/MM optimizations; the surrounding protein environment was considered as the MM whose atomistic coordinates were exactly fixed with the original X-ray coordinates. After obtaining the stable geometry of QM fragment, we then determined the ESP charges for the cationic state of $[P_{D1}/P_{D2}]^{\bullet+}$ Chl dimer in the presence of the entire PSII atomic coordinates (Table S1, supporting information).

3. Results and discussion

3.1. Orientation of the formyl group in Chl*d*

Chl*d* molecules at the P_{D1}/P_{D2} position were modeled by replacing the vinyl group of Chl*a* in the *T. vulcanus* PSII crystal structure with a formyl group. The position of this newly-introduced formyl group of Chl*d* was refined by the constrained QM/MM optimizations in the PSII protein environment as described above. Two orientations of the formyl group were energetically stable; one with the carbonyl O atom being oriented to the C5 H atom (Fig. 2a) and another one with the formyl group flipped along the C3–$C3^1$ axis (Fig. 2b).

The former orientation was slightly (by ~3 kcal/mol) more stable than the latter the monomeric form of Chl*d* in vacuum. In contrast, in

the PSII protein environment, the latter orientation was always slightly (by ~3 kcal/mol) more stable than the former in all cases investigated, i.e., the dimeric form (Chl*a*/Chl*a*, Chl*d*/Chl*a*, and Chl*d*/Chl*d*). Hence, the conformer in Fig. 2a is advantageous in terms of intramolecular interaction energy (i.e., monomeric Chl itself) because the negative charge of the formyl O atom can be more stabilized by the proximity of the positive charge of the C5 H atom. On the other hand, in the P_{D1}/P_{D2} pair, the conformer in Fig. 2b appears to be slightly advantageous in terms of the intermolecular energy (i.e., interaction with another Chl. We will not focus on elucidation of further details in the present study.). Thus, we focused on the latter orientation of the Chl*d* formyl group (Fig. 2a) to investigate the cationic state distribution over the P_{D1}/P_{D2} pair in the PSII protein environment.

The formyl groups of P_{D1} and P_{D2} were located at a van der Waals distance (~3.5 Å) from D1-Met183/D2-Leu182 and D1-Phe206/D2-Leu206 in the geometry of the *T. vulcanus* PSII (Table S1, supporting information). These residue pairs correspond to Met/Leu and Leu/Leu in the D1/D2 protein sequences of the *A. marina* PSII, respectively (Fig. S1, supporting information). Although it has been reported that the presence of an H bond partner for Chl affects the distribution of the cationic (spin) state over the Chl pair (e.g., in PSI [25,50]), the present analysis suggests that the formyl groups will not possess H-bond partners in the *A. marina* PSII.

3.2. $P_{D1}^{\bullet+}/P_{D2}^{\bullet+}$ ratio

Tomo et al. proposed that the P_{D1}/P_{D2} pair in the *A. Marina* PSII was composed of a Chl*d*/Chl*d* pair [36]. The corresponding calculated $P_{D1}^{\bullet+}/P_{D2}^{\bullet+}$ ratio for the Chl*d*/Chl*d* pair was 76.5/23.5 in the whole PSII (Table 1), which is essentially the same as that of the Chl*a*/Chl*a* pair previously reported for the *T. vulcanus* PSII (76.9/23.1 [24]). The Chl*a*/Chl*d* pair, which was proposed by Schlodder et al. as the P_{D1}/P_{D2} pair in the *A. Marina* PSII [31], also resulted in a similar $P_{D1}^{\bullet+}/P_{D2}^{\bullet+}$ ratio of 85.1/14.9 (Table 1).

On the other hand, the Chl*d*/Chl*a* pair resulted in a $P_{D1}^{\bullet+}/P_{D2}^{\bullet+}$ ratio of approximately 50/50 (Table 1). Such a ratio was not proposed by Tomo et al. [36] or Schlodder et al. [31]. Because the cationic state distribution over the Chl pair is associated with the redox potentials for the E_m of the 2 Chl monomers [24,25,51,52], similar amounts for the $P_{D1}^{\bullet+}$ and $P_{D2}^{\bullet+}$ populations imply that the E_m values of the 2 monomeric P_{D1} (Chl*d*) and P_{D2} (Chl*a*) Chls are also similar. The experimentally measured E_m value for Chl*d* in DMF is approximately 70 mV higher than that of Chl*a* [39]. This E_m difference between Chl*d* and Chl*a* is almost in the same range as the E_m difference between P_{D1} and P_{D2}, previously measured as 70–100 mV in the *T. vulcanus* PSII [24]. Thus, a Chl*d*/Chl*a* pair should yield isoenergetic E_m values for the 2 monomeric Chls. Thus, we can conclude that the Chl*d*/Chl*a* pair is unlikely to represent the P_{D1}/P_{D2} pair in the *A. marina* PSII.

Hence, it appears that both the Chl*d*/Chl*d* pair [36] and the Chl*a*/Chl*d* pair [31] are still possible candidates for the P_{D1}/P_{D2} pair in the *A. Marina* PSII. The reported localization of approximately 70–80% of the cationic state on P_{D1} in FTIR studies by Tomo et al. [36,37] is in accordance with the calculated $P_{D1}^{\bullet+}/P_{D2}^{\bullet+}$ ratio for the Chl*d*/Chl*d* pair in the present study (Table 1). However, the observed cationic state localization on a single Chl*a* that was attributed to P_{D1} in studies by Schlodder et al. [31] also agrees with our calculated $P_{D1}^{\bullet+}/P_{D2}^{\bullet+}$ ratio for the Chl*a*/Chl*d* pair (Table 1). These subtle differences in the $P_{D1}^{\bullet+}/P_{D2}^{\bullet+}$ ratios between the Chl*d*/Chl*d* pair and the Chl*a*/Chl*d* pair still make it difficult to determine the configuration of the relevant Chl pair in the *A. marina* PSII.

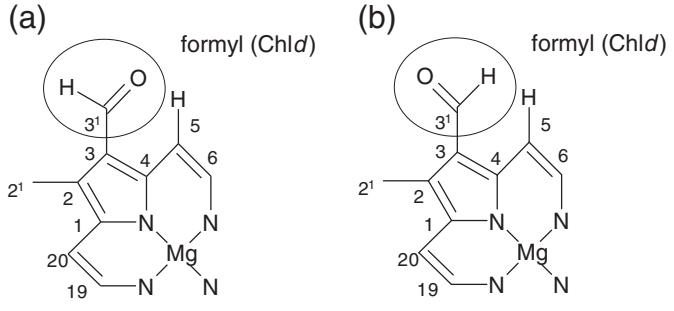

Fig. 2. Possible orientations of the formyl group in Chl*d*; (a) one with the carbonyl O atom being oriented to the C5 H atom and (b) another one with the formyl group flipped along the C3–C3^1 axis.

Table 1
Calculated values (%) for the $P_{D1}^{\bullet+}/P_{D2}^{\bullet+}$ ratio and spin density distribution in the D1/D2 subunit of the *Thermosynechococcus vulcanus* PSII [42].

	Charge		Spin	
	$P_{D1}^{\bullet+}$	$P_{D2}^{\bullet+}$	P_{D1}	P_{D2}
[whole PSII]				
Chl*a*/Chl*a* (*T. vulcanus*[a])	76.9	23.1	80.1	19.9
Chl*d*/Chl*d* (Tomo et al.[b])	76.5	23.5	85.1	14.9
Chl*a*/Chl*d* (Schlodder et al.[c])	85.1	14.9	95.2	4.8
Chl*d*/Chl*a*	56.7	43.3	55.8	44.2

[a] See Ref. [24].
[b] See Refs. [36,37].
[c] See Ref. [31].

4. Conclusions

$P_{D1}^{\bullet+}/P_{D2}^{\bullet+}$ ratios for the Chl*d*/Chl*d* pair or the Chl*a*/Chl*d* pair in the *T. vulcanus* PSII environment were calculated to be 76.5/23.5 or 85.1/14.9, respectively, rendering a large $P_{D1}^{\bullet+}$ population relative to the $P_{D2}^{\bullet+}$ population. On the other hand, the Chl*d*/Chl*a* pair resulted in a symmetrically charged population over the two P_{D1} and P_{D2} monomers (56.7/43.3). The present results strongly suggest that the Chl*d*/Chl*a* pair is unlikely to serve as P_{D1}/P_{D2} in *A. marina* PSII. Further detailed studies, preferably on crystal structures of the *A. marina* PSII are required to unambiguously confirm the P_{D1}/P_{D2} pair to be either Chl*d*/Chl*d* or Chl*a*/Chl*d*.

Acknowledgements

This research was supported by the JST PRESTO program (H.I), Grant-in-Aid for Scientific Research from the Ministry of Education, Culture, Sports, Science and Technology (MEXT) of Japan (21770163 to H.I. and 22740276 to K.S.), Special Coordination Fund (H.I.) for Promoting Science and Technology of MEXT, Takeda Science Foundation (H.I.), Kyoto University Step-up Grant-in-Aid for young scientists (H. I.), and Grant for Basic Science Research Projects from The Sumitomo Foundation (H. I.).

References

[1] V.I. Prokhorenko, A.R. Holzwarth, Primary process and structure of the photosystem II reaction center: a photon echo study, J. Phys. Chem. B 104 (2000) 11563–11578.
[2] B.A. Diner, F. Rappaport, Structure dynamics, and energetics of the primary photochemistry of photosystem II of oxygenic photosynthesis, Annu. Rev. Plant Biol. 53 (2002) 551–580.
[3] G. Renger, T. Renger, Photosystem II: the machinery of photosynthetic water splitting, Photosynth. Res. 98 (2008) 53–80.
[4] V.V. Klimov, S.I. Allakhverdiev, S. Demeter, A.A. Krasnovskii, Photoreduction of pheophytin in the photosystem 2 of chloroplasts with respect to the redox potential of the medium, Dokl. Akad. Nauk SSSR 249 (1979) 227–230.
[5] A.W. Rutherford, J.E. Mullet, A.R. Crofts, Measurement of the midpoint potential of the pheophytin acceptor of photosystem II, FEBS Lett. 123 (1981) 235–237.
[6] T. Watanabe, M. Kobayashi, Electrochemistry of chlorophylls, in: H. Scheer (Ed.), Chlorophylls, CRC Press, Boca Raton, FL, 1991, pp. 287–303.
[7] S. Ohashi, T. Iemura, H. Miyashita, T. Watanabe, M. Kobayashi, New scheme for O_2 evolution in PSII, Photomed. Photobiol. 30 (2008) 13–18.
[8] M. Kobayashi, S. Ohashi, S. Fukuyo, M. Kasahara, T. Watanabe, The oxidation potential of Chl*a* is the lowest: a new scheme for O_2 evolution in PSII, in: J.F. Allen, E. Gantt, J.H. Golbeck, B. Osmond (Eds.), Photosynthesis: Energy from the Sun, Springer, 2008, pp. 113–116.

[9] A. Zouni, H.T. Witt, J. Kern, P. Fromme, N. Krauss, W. Saenger, P. Orth, Crystal structure of photosystem II from *Synechococcus elongatus* at 3.8 Å resolution, Nature 409 (2001) 739–743.

[10] F. Rappaport, M. Guergova-Kuras, P.J. Nixon, B.A. Diner, J. Lavergne, Kinetics and pathways of charge recombination in photosystem II, Biochemistry 41 (2002) 8518–8527.

[11] A. Krieger, A.W. Rutherford, G.N. Johnson, On the determination of redox midpoint potential of the primary quinone electron transfer acceptor, Q_A, in photosystem II, Biochim. Biophys. Acta 1229 (1995) 193–201.

[12] G.N. Johnson, A.W. Rutherford, A. Krieger, A change in the midpoint potential of the quinone Q_A in Photosystem II associated with photoactivation of oxygen evolution, Biochim. Biophys. Acta 1229 (1995) 202–207.

[13] M. Grabolle, H. Dau, Energetics of primary and secondary electron transfer in photosystem II membrane particles of spinach revisited on basis of recombination-fluorescence measurements, Biochim. Biophys. Acta 1708 (2005) 209–218.

[14] B. Loll, J. Kern, W. Saenger, A. Zouni, J. Biesiadka, Towards complete cofactor arrangement in the 3.0 Å resolution structure of photosystem II, Nature 438 (2005) 1040–1044.

[15] H. Ishikita, W. Saenger, J. Biesiadka, B. Loll, E.-W. Knapp, How photosynthetic reaction centers control oxidation power in chlorophyll pairs P680, P700 and P870, Proc. Natl. Acad. Sci. U. S. A. 103 (2006) 9855–9860.

[16] Y. Kato, M. Sugiura, A. Oda, T. Watanabe, Spectroelectrochemical determination of the redox potential of pheophytin *a*, the primary electron acceptor in photosystem II, Proc. Natl. Acad. Sci. U. S. A. 106 (2009) 17365–17370.

[17] G. Renger, A.R. Holzwarth, Plastoquinone oxido-reductase in photosynthesis, in: T. Wydrqynski, K. Satoh (Eds.), Photosystem II, Springer, Dordrecht, The Netherlands, 2005, pp. 139–175.

[18] G. Renger, in: G. Renger (Ed.), Primary Processes of Photosynthesis: Principles and Apparatus, Part II, Royal Society Chemistry, Cambridge, UK, 2008, pp. 237–290.

[19] H. Dau, M. Haumann, The manganese complex of photosystem II in its reaction cycle? Basic framework and possible realization at the atomic level, Coord. Chem. Rev. 252 (2008) 273–295.

[20] F. Rappaport, B.A. Diner, Primary photochemistry and energetics leading to the oxidation of the Mn_4Ca cluster and to the evolution of molecular oxygen in photosystem II, Coord. Chem. Rev. 252 (2008) 259–272.

[21] S.E.J. Rigby, J.H.A. Nugent, P.J. O'Malley, ENDOR and special triple resonance studies of chlorophyll cation radicals in photosystem 2, Biochemistry 33 (1994) 10043–10050.

[22] B.A. Diner, E. Schlodder, P.J. Nixon, W.J. Coleman, F. Rappaport, J. Lavergne, W.F.J. Vermaas, D.A. Chisholm, Site-directed mutations at D1-His198 and D2-His197 of photosystem II in *Synechocystis* PCC 6803: sites of primary charge separation and cation and triplet stabilization, Biochemistry 40 (2001) 9265–9281.

[23] H. Michel, J. Deisenhofer, Relevance of the photosynthetic reaction center from purple bacteria to the structure of photosystem II, Biochemistry 27 (1988) 1–7.

[24] K. Saito, T. Ishida, M. Sugiura, K. Kawakami, Y. Umena, N. Kamiya, J.-R. Shen, H. Ishikita, Distribution of the cationic state over the chlorophyll pair of photosystem II reaction center, J. Am. Chem. Soc. 133 (2011) 14379–14388.

[25] K. Saito, H. Ishikita, Cationic state distribution over the P700 chlorophyll pair in photosystem I, Biophys. J. 101 (2011) 2018–2025.

[26] M. Akiyama, H. Miyashita, H. Kise, T. Watanabe, M. Mimuro, S. Miyachi, M. Kobayashi, Quest for minor but key chlorophyll molecules in photosynthetic reaction centers — unusual pigment composition in the reaction centers of the chlorophyll *d*-dominated cyanobacterium *Acaryochloris marina*, Photosynth. Res. 74 (2002) 97–107.

[27] M. Mimuro, S. Akimoto, T. Gotoh, M. Yokono, M. Akiyama, T. Tsuchiya, H. Miyashita, M. Kobayashi, I. Yamazaki, Identification of the primary electron donor in PS II of the Chl *d*-dominated cyanobacterium *Acaryochloris marina*, FEBS Lett. 556 (2004) 95–98.

[28] M. Chen, A. Telfer, S. Lin, A. Pascal, A.W. Larkum, J. Barber, R.E. Blankenship, The nature of the photosystem II reaction centre in the chlorophyll *d*-containing prokaryote, *Acaryochloris marina*, Photochem. Photobiol. Sci. 4 (2005) 1060–1064.

[29] W.D. Swingley, M.F. Hohmann-Marriott, T. Le Olson, R.E. Blankenship, Effect of iron on growth and ultrastructure of *Acaryochloris marina*, Appl. Environ. Microbiol. 71 (2005) 8606–8610.

[30] S.I. Allakhverdiev, T. Tomo, Y. Shimada, H. Kindo, R. Nagao, V.V. Klimov, M. Mimuro, Redox potential of pheophytin a in photosystem II of two cyanobacteria having the different special pair chlorophylls, Proc. Natl. Acad. Sci. U. S. A. 107 (2010) 3924–3929.

[31] E. Schlodder, M. Cetin, H.J. Eckert, F.J. Schmitt, J. Barber, A. Telfer, Both chlorophylls *a* and *d* are essential for the photochemistry in photosystem II of the cyanobacteria, *Acaryochloris marina*, Biochim. Biophys. Acta 1767 (2007) 589–595.

[32] M. Sugiura, F. Rappaport, K. Brettel, T. Noguchi, A.W. Rutherford, A. Boussac, Site-directed mutagenesis of *Thermosynechococcus elongatus* photosystem II: the O_2-evolving enzyme lacking the redox-active tyrosine D, Biochemistry 43 (2004) 13549–13563.

[33] T. Okubo, T. Tomo, M. Sugiura, T. Noguchi, Perturbation of the structure of P680 and the charge distribution on its radical cation in isolated reaction center complexes of photosystem II as revealed by Fourier transform infrared spectroscopy, Biochemistry 46 (2007) 4390–4397.

[34] T. Renger, E. Schlodder, The primary electron donor of photosystem II of the cyanobacterium *Acaryochloris marina* is a chlorophyll *d* and the water oxidation is driven by a chlorophyll *a*/chlorophyll *d* heterodimer, J. Phys. Chem. B 112 (2008) 7351–7354.

[35] K. Cser, Z. Deak, A. Telfer, J. Barber, I. Vass, Energetics of photosystem II charge recombination in *Acaryochloris marina* studied by thermoluminescence and flash-induced chlorophyll fluorescence measurements, Photosynth. Res. 98 (2008) 131–140.

[36] T. Tomo, T. Okubo, S. Akimoto, M. Yokono, H. Miyashita, T. Tsuchiya, T. Noguchi, M. Mimuro, Identification of the special pair of photosystem II in a chlorophyll *d*-dominated cyanobacterium, Proc. Natl. Acad. Sci. U. S. A. 104 (2007) 7283–7288.

[37] T. Tomo, S.I. Allakhverdiev, M. Mimuro, Constitution and energetics of photosystem I and photosystem II in the chlorophyll d-dominated cyanobacterium *Acaryochloris marina*, J. Photochem. Photobiol. B 104 (2011) 333–340.

[38] S.I. Allakhverdiev, T. Tsuchiya, K. Watabe, A. Kojima, D.A. Los, T. Tomo, V.V. Klimov, M. Mimuro, Redox potentials of primary electron acceptor quinone molecule $(Q_A)^-$ and conserved energetics of photosystem II in cyanobacteria with chlorophyll *a* and chlorophyll *d*, Proc. Natl. Acad. Sci. U. S. A. 108 (2011) 8054–8058.

[39] M. Kobayashi, S. Ohashi, K. Iwamoto, Y. Shiraiwa, Y. Kato, T. Watanabe, Redox potential of chlorophyll *d in vitro*, Biochim. Biophys. Acta 1767 (2007) 596–602.

[40] V. Sivakumar, R. Wang, G. Hastings, Photo-oxidation of P740, the primary electron donor in photosystem I from *Acaryochloris marina*, Biophys. J. 85 (2003) 3162–3172.

[41] G. Hastings, R. Wang, Vibrational mode frequency calculations of chlorophyll-*d* for assessing ($P740^+$–P740) FTIR difference spectra obtained using photosystem I particles from *Acaryochloris marina*, Photosynth. Res. 95 (2008) 55–62.

[42] Y. Umena, K. Kawakami, J.-R. Shen, N. Kamiya, Crystal structure of oxygen-evolving photosystem II at 1.9 Å resolution, Nature 473 (2011) 55–60.

[43] M. Mimuro, S. Akimoto, I.I. Yamazaki, H. Miyashita, S. Miyachi, Fluorescence properties of chlorophyll *d*-dominating prokaryotic alga, *Acaryochloris marina*: studies using time-resolved fluorescence spectroscopy on intact cells, Biochim. Biophys. Acta 1412 (1999) 37–46.

[44] B.R. Brooks, R.E. Bruccoleri, B.D. Olafson, D.J. States, S. Swaminathan, M. Karplus, CHARMM: a program for macromolecular energy minimization and dynamics calculations, J. Comput. Chem. 4 (1983) 187–217.

[45] A.D. MacKerell Jr., D. Bashford, R.L. Bellott, R.L. Dunbrack Jr., J.D. Evanseck, M.J. Field, S. Fischer, J. Gao, H. Guo, S. Ha, D. Joseph-McCarthy, L. Kuchnir, K. Kuczera, F.T.K. Lau, C. Mattos, S. Michnick, T. Ngo, D.T. Nguyen, B. Prodhom, W.E. Reiher III, B. Roux, M. Schlenkrich, J.C. Smith, R. Stote, J. Straub, M. Watanabe, J. Wiorkiewicz-Kuczera, D. Yin, M. Karplus, All-atom empirical potential for molecular modeling and dynamics studies of proteins, J. Phys. Chem. B 102 (1998) 3586–3616.

[46] B. Rabenstein, G.M. Ullmann, E.-W. Knapp, Calculation of protonation patterns in proteins with structural relaxation and molecular ensembles — application to the photosynthetic reaction center, Eur. Biophys. J. 27 (1998) 626–637.

[47] K. Kanda, S. Yamanaka, T. Saito, Y. Umena, K. Kawakami, J.-R. Shen, N. Kamiya, M. Okumura, H. Nakamura, K. Yamaguchi, Labile electronic and spin states of the $CaMn_4O_5$ cluster in the PSII system refined to the 1.9 Å X-ray resolution. UB3LYP computational results, Chem. Phys. Lett. 506 (2011) 98–103.

[48] S. Luber, I. Rivalta, Y. Umena, K. Kawakami, J.-R. Shen, N. Kamiya, G.W. Brudvig, V.S. Batista, S_1-state model of the O_2-evolving complex of photosystem II, Biochemistry 50 (2011) 6308–6311.

[49] QSite, version 5.6, Schrödinger, LLC, New York, NY, 2010.

[50] Y. Li, M.-G. Lucas, T. Konovalova, B. Abbott, F. MacMillan, A. Petrenko, V. Sivakumar, R. Wang, G. Hastings, F. Gu, J. van Tol, L.-C. Brunel, R. Timkovich, F. Rappaport, K. Redding, Mutation of the putative hydrogen-bond donor to P_{700} of photosystem I, Biochemistry 43 (2004) 12634–12647.

[51] F. Muh, F. Lendzian, M. Roy, J.C. Williams, J.P. Allen, W. Lubitz, Pigment–protein interactions in bacterial reaction centers and their influence on oxidation potential and spin density distribution of the primary donor, J. Phys. Chem. B 106 (2002) 3226–3236.

[52] H. Witt, E. Schlodder, C. Teutloff, J. Niklas, E. Bordignon, D. Carbonera, S. Kohler, A. Labahn, W. Lubitz, Hydrogen bonding to P700: site-directed mutagenesis of threonine A739 of photosystem I in *Chlamydomonas reinhardtii*, Biochemistry 41 (2002) 8557–8569.